IOSR Journal of Engineering (IOSRJEN) **www.iosrjen.org**
ISSN (e): 2250-3021, ISSN (p): 2278-8719
Vol. 09, Issue 6 (June. 2019), ||S (I) || PP 28-34

ZnO Nanorods and its Photocatalytic Studies on Methylene Blue Dye

D. Nathiya[1], N.M.I. Alhaji[1*], A. M. Uduman Mohideen[1], A. Ayeshamariam[2]
[1]*Department of Chemistry, Khadir Mohideen College, Adirampattinam, 614701, India.*
[2]*Department of Physics, Khadir Mohideen College, Adirampattinam, 614701, India.*
**Corresponding Author: N.M.I. Alhaji*

Abstract: Flower-shaped ZnO NPs were synthesized directly from an aqueous solution of zinc nitrate in the presence of CTAB at 140 °C. The as-synthesized products were investigated in terms of their morphological, structural, photocatalytic properties. Methylene blue (MB) is employed to evaluate the photocatalytic activity of the ZnO NPs. The photocurrent response experiments are also carried out. The as-formed composite shows higher efficiency of photocatalytic degradation on MB. Moreover, it also exhibits obvious photodegradation under light irradiation.

Keywords: ZnO NPs, hydrothermal and photocatalytic degradation

---

Date of Submission: 25-05-2019 Date of acceptance: 10-06-2019

I. INTRODUCTION

Most important of all, we hope to unify some often-utilizing concepts surrounding the keyword of photocatalysis and provide the usage to focus on the important common scientific merits of seemingly different approaches [1]. ZnO exhibits superior photocatalytic activity owing to its higher efficiency in generating, moving and separating photoinduced electrons and holes. Thus, ZnO is widely used in the removal of toxic, harmful or hazardous organic pollutants from sewage in industrial water treatment [2]. Meanwhile, the modification of semiconductors with noble metals has attracted significant attention. It is found that catalytic noble metals, such as Ag nanorods, can improve the surface states of ZnO nanocrystals. In another words, Ag and oxygen vacancy defects on the ZnO surface can trap the photo generated electrons from the semiconductor, and benefit the separation of photogenerated electron–hole pairs, thus enhancing the photocatalytic activity. Aligned ZnO nanowires on pre-seeded silicon, glass, and gallium nitride substrates have been grown using aqueous zinc salts such as zinc nitrate and zinc acetate in basic environments. Pre-seeding substrates with ZnO creates sites for homogeneous nucleation of ZnO crystal during the synthesis. Common pre-seeding methods include in-situ thermal decomposition of zinc acetate crystallites, spincoating of ZnO nanorods and the use of physical vapour deposition methods to deposit ZnO thin films. Pre-seeding can be performed in conjunction with top down patterning methods such as electron beam lithography and nanosphere lithography to designate nucleation sites prior to growth. Aligned ZnO nanowires can be used in dye-senitized solar cells and field emission devices [3]. In general, the metal–semiconductor nanocomposites are prepared by two-step method. The four most common face terminations of wurtzite ZnO are the polar Zn terminated (0001) and O terminated (000.1) faces (*c*-axis oriented), and the non-polar (11.20) (*a*-axis) and (10.10) faces which both contain an equal number of Zn and O atoms. The polar faces are known to possess different chemical and physical properties, and the O-terminated face possess a slightly different electronic structure to the other three faces [4]. In this paper, we succeeded in synthesizing ZnO NPs by the hydrothermal synthesis using $Zn(NO_3)_2{\cdot}6H_2O$ in the presence of (CTAB). The catalytic efficiency was evaluated by degradation of methylene blue (MB) under UV irradiation, and the degradation extent can be easily detected by gas chromatograph and the UV–vis spectrophotometer. The relationship between the photocatalytic activity and the structural features of the prepared catalysts was investigated through a systematic characterization analysis, and a possible mechanism of the reaction was proposed [5].

II. EXPERIMENTAL

2.1. Preparation and characterization

ZnO NPs were synthesized by simple hydrothermal process. In a typical procedure, 0.016 M $Zn(NO_3)_2{\cdot}6H_2O$, 0.5 M hexadecyl trimethylammonium bromide (CTAB) and 0.25 M NaOH were in turn dissolved in 10 mL of distilled water with continuous stirring until a homogeneous solution was obtained. 10 mL ethylene glycol was then added into the above solution under continuous stirrring for 10 min at room-

temperature. The final solution was consequently transferred to teflon lined autoclave which was then sealed and heated upto 120 °C for 6 h. After being cooled to room temperature, these precipitates were filtered, rinsed with distilled water several times, then dried at 50 °C [6]. The structural characterization of the ZnO powders was carried out by the X-ray diffractometer (XRD; RIGAKU/DMAX2500,Tokyo, Japan) using Cu Kα radiation with the wavelength of 0.15406 nm. Morphological studies used a scanning electron microscope (SEM, Quanta 400, FEI) and transmission electron microscope (TEM, JEM 2010, JEOL). The UV-Vis diffuse reflectance spectra were recorded on a uv–vis spectrophotometer (UV-2450, Shimadzu) using $BaSO_4$ as a reference. The total surface areas of the samples were determined by the Brunauer-Emmett-Teller (BET) method using the surface area analyzer (Autosorb 1 MP, Quantachrome).

2.2. Photocatalytic degradation

Methylene blue was employed to evaluate the photocatalytic activity of the ZnO NPs. A mixture of 40 mL of 1.0×10^{-5} M dye aqueous solution and 150 mg of ZnO powders was stirred for 30 min in the dark to ensure that the adsorption/desorption of the dye on the ZnO surface was in equilibrium. Then the mixture was irradiated using an irradiation from a Xe lamp (CHF-XM-500W, Chang Tuo Sci-tech, Beijing). 2 mL of the dye solution was collected after irradiation times and centrifuged to separate the ZnO powders. The integrated visible-light intensity was measured to be 25 mW/cm^2 using a visible light radiometer (FZ-A). The remaining dye concentration was determined by measuring the absorption with a UV–vis spectrophotometer (lambda 25, Perkin Elmer). The degradation or decolorization efficiency was calculated according to the equation:

$$Degradation\ (\%)=(C_0-C)/C_0$$

where C_0 and C are the initial and changed concentrations of MB dye, respectively.

The photocatalytic activities of the prepared ZnO were evaluated by measuring the decomposition MB under visible light irradiation. Before irradiation, the reactor was kept in the dark for 40 min to ensure an adsorption desorption equilibrium of gaseous reactants on the sample. Then the reactor was irradiated using a visible light for 2 h at room temperature. The reaction products were measured using a gas chromatograph (GC-14B, Shimadzu) equipped with a flame ionization detector.

III. RESULTS AND DISCUSSION

3.1. Characterization of Photocatalayst

To examine the structural properties and crystal phase identifications, powder X-ray diffraction (XRD) was measured with Cu-Kradiation in the range of 10–80º. Figure 1 displays the XRD pattern of the ZnO NPs. The observed XRD pattern exhibits well crystalline nature and mixed phases of ZnO NPs for as-synthesized NPs. Several well-defined diffraction reflections are consistent with the values in the standard card small peaks corresponding to ZnO (1 0 0) and (1 0 1) are also appeared at 31.9 and 36.12° (JCPDS file no. 36-1451). Except ZnO, no other reflections related to impurities such as Zn and O were found in the pattern [7]. Hexagonal structure and have a preferential growth along the [10 0] orientation along the c-axis which effectively lowered the nucleation energy barrier and heterogeneous nucleation and its hexagonal structure is shown in Figure 2. Structural parameter values are shown in Table-1. The calculated crystal size was nearly 36 nm.

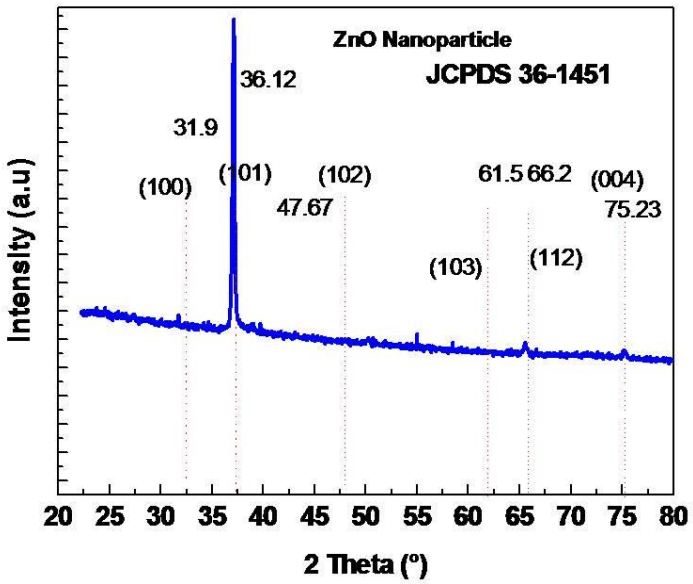

Figure 1 XRD analysis of ZnO NPs

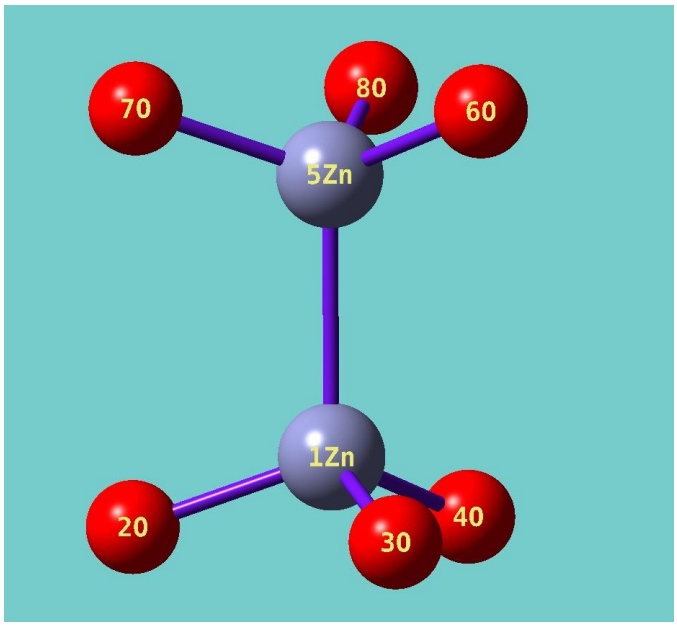

Figure 2 Structural studies of ZnO NPs

Table 1 Strutural analysis of ZnO NPs

Position 2Θ(Std)	Position 2Θ (obs)	d-sapcing (std)	d-sapcing (obs)	FWHM [°2Th.]	Relative Intensity	Lattice parameters Aº(JCPDS)	Lattice parameters Aº(cal)	hkl planes
36.253	36.12	2.4759	2.471	0.144	100	Hexagonal - **P 63mC**		101
47.539	47.67	1.9110	1.900	1.224	8.20	a = 3.249	a = 3.215	102
66.380	66.20	1.4071	1.412	0.310	6.55	c = 5.206	c = 5.192	200
75.562	75.23	1.3017	1.299	1.300	5.25			004

The morphologies of as-synthesized ZnO NPs were investigated by using FE-SEM and results are shown in Figure 3a. It can be clearly seen in Figure 3(a) that the ZnO NPs are self-assembled together to form rod like structure. The typical dimension of a single flower is about 400 ± 50 nm [8]. A magnified FESEM image of ZnO NPs for clarity of its morphology, Figure 3b of EDAX results shows that prepared powdered particle is free from impurity. Its composition results are shown in Table 2. In SEM analysis the particles are agglomerated so its size is nearly in micrometer.

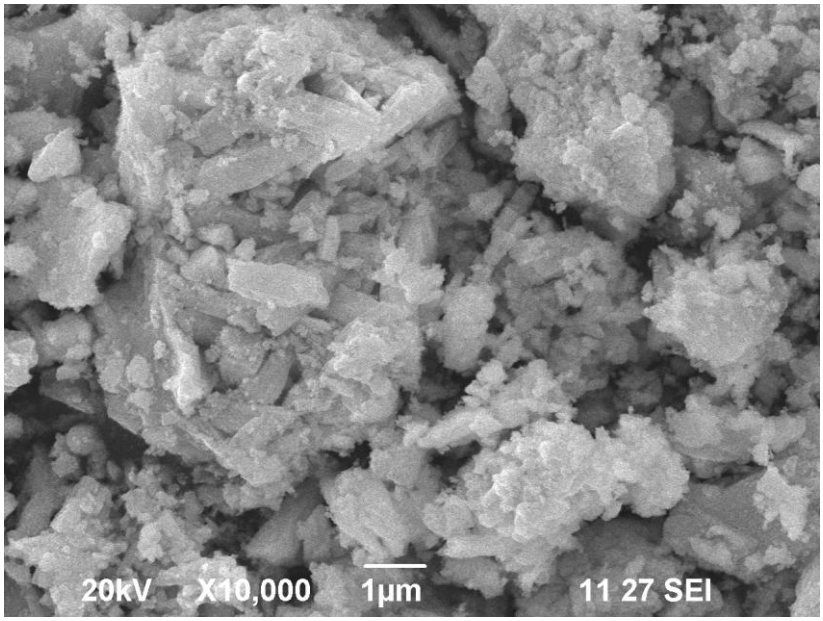

Figure 3a SEM analysis of ZnO NPs prepared by using hydrothermal method

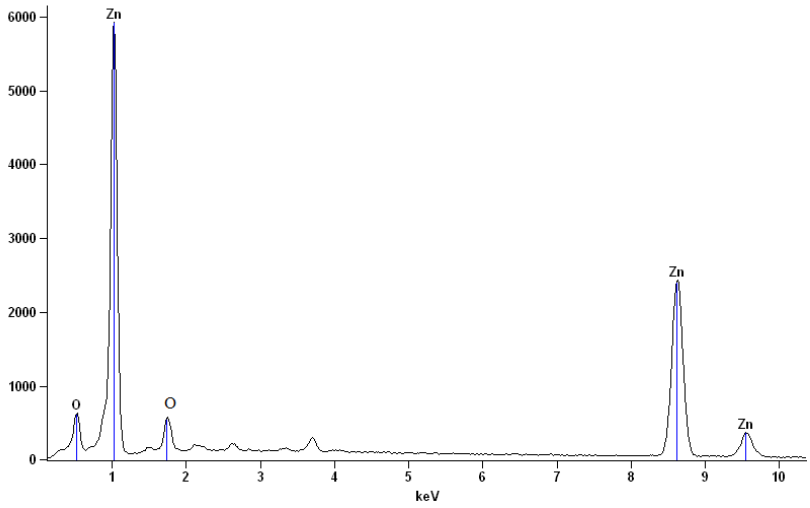

Figure 3b. EDAX Analysis of ZnO

Table 2. EDAX Analysis of ZnO

Element	*Net Counts*	*ZAF*	*Weight %*	*Atom %*	*Formula*
O	4683	3.414	18.37	45.78	O
O	5259	3.246	5.49	7.79	O
Zn	48015	1.062	76.14	46.43	Zn
Total			100.00	100.00	

TEM images were further taken to investigate the detailed structure of the ZnO NPs. Figure 4(a) shows a low-magnified TEM image of the sample. The as-synthesized composites are made up of several plates and nanorods. These rods with wider bases are connected with each other in such a special fashion that they make flower-like morphologies. A high-magnified TEM images of an individual ZnO plate are shown in Figures 4(a), where clear lattice fringes can be observed. Figure 4(b) shows that the selected area electron diffraction (SAED) pattern are fairly close to those of the (1 0 0) and (0 0 2) plane of ZnO [9].

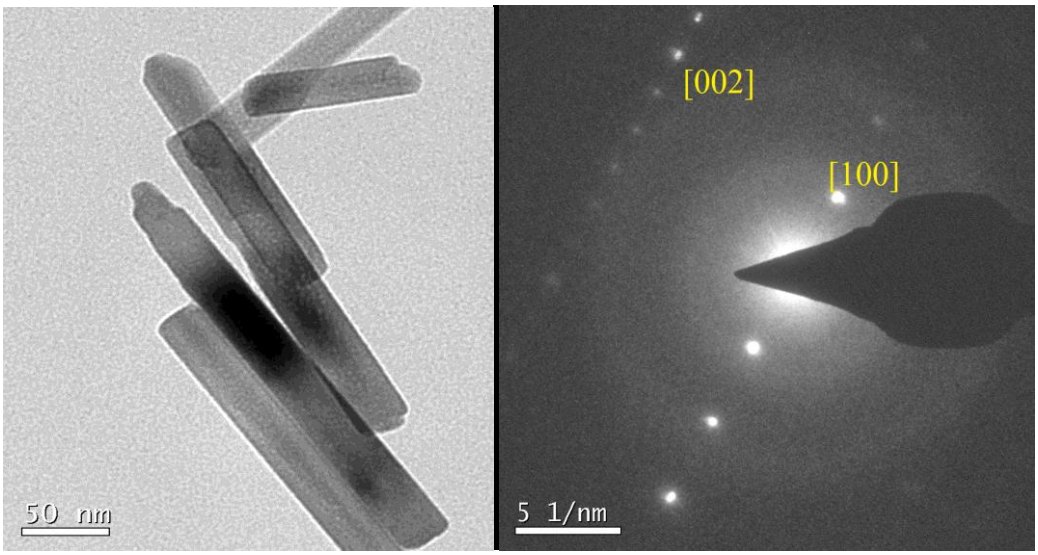

Figure 4 (a-b) TEM images of ZnO nanorods and its SAED pattern

Figure 5(a) shows the UV-vis absorption spectra of ZnO NPs. There are two absorption bands at 360 and at 470 nm in the absorption spectra. Absorption band at 360 nm is due to transition of electrons from valance band to conduction band, which is the intrinsic absorption band of ZnO NPs. The absorption peak at 470 nm can be ascribed ZnO nanorods structure [10]

The specific surface areas of the ZnO NPs have been evaluated based upon N_2 adsorption/desorption experiments. Figure 5b shows the N_2 dsorption/desorption isotherms for the sample. The absence of a sharp rise

in nitrogen uptake near the saturation pressure (i.e., P/P_0=1) means that there are few macropores in the samples [11]. The Brunauer-Emmett-Teller (BET) surface areas of the samples are determined to be 24 m^2 g^{-1}.

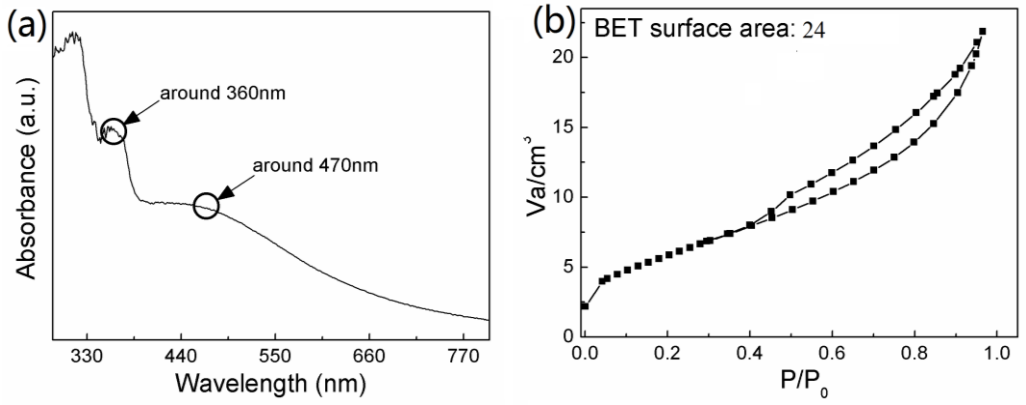

Figure 5(a-b) Absorbance and Adsorption surface area of ZnO NPs

3.2. Photocatalytic activities

In order to evaluate the photocatalytic activities of the ZnO NPs, methylene blue dye solution is chosen to be decomposed under irradiation. Figure 6(a) shows the photocatalytic degradation of MB as a function of irradiation times on ZnO powders. In dark test (0 min), a small adsorption and desorption of MB on catalyst powder can be observed. This means that the concentration of MB has attained saturation and the adsorption equilibrium was reached. When the light was turned on, the MB would be photodecomposed gradually. The degradation efficiency of 98% with ZnO can be reached at 60 min of irrdiation time.

Besides the photodegradation of the MB dye solutions was selected to evaluate the photocatalytic mineralization on the ZnO catalyst, Figure 6(b) shows the photocatalytic decomposition of ZnO under visible light ($\lambda \geq 400$ nm) irradiation. When the light is turned on, the acetone and CO_2 are produced gradually; the evolution yield can reached 500 and 70 *ppm* under visible light irradiation. Under visible light irradiation, the electron and hole are generated and then transformed to the surface of ZnO rods. This can effectively inhibit the electron–hole recombination or charge recombination and therefore enhance the photocatalytic activity [12]

Besides the photodegradation of the MB dye solutions, was selected to evaluate the Photocatalytic mineralization on the ZnO powder was shown in Figure 6 (a-c) under visible light ($\lambda \geq 400$ nm) irradiation. The absorbance curves shows the peak values for ZnO(547 nm). Like that Photocatalytic studies of variation of Time (min) Vs with (C/C_0) of ZnO was studied and plotted in Figure 6a. Under visible light irradiation, the electron and hole are generated and then transformed to the surface of ZnO nanorods [13]. What the effects of ZnO nanorods is to collect photogenerated electrons from the conduction band of ZnO nanorods and improve charge separation in semiconductor-metal composite systems. This can effectively inhibit the electron–hole recombination or charge recombination and therefore enhance the Photocatalytic activity. Its kinetic parameters values are shown in Table 3.

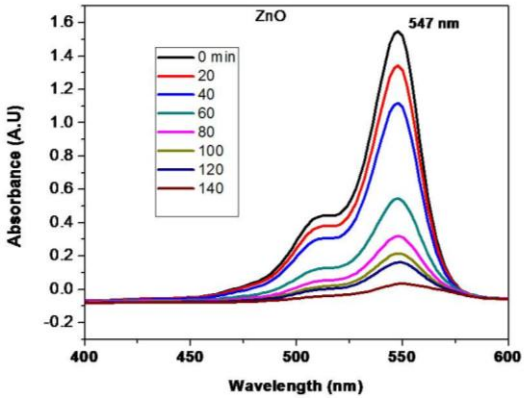

Figure 6a Absorbance values of methylene blue (MB) dye as catalyst in ZnO solutions

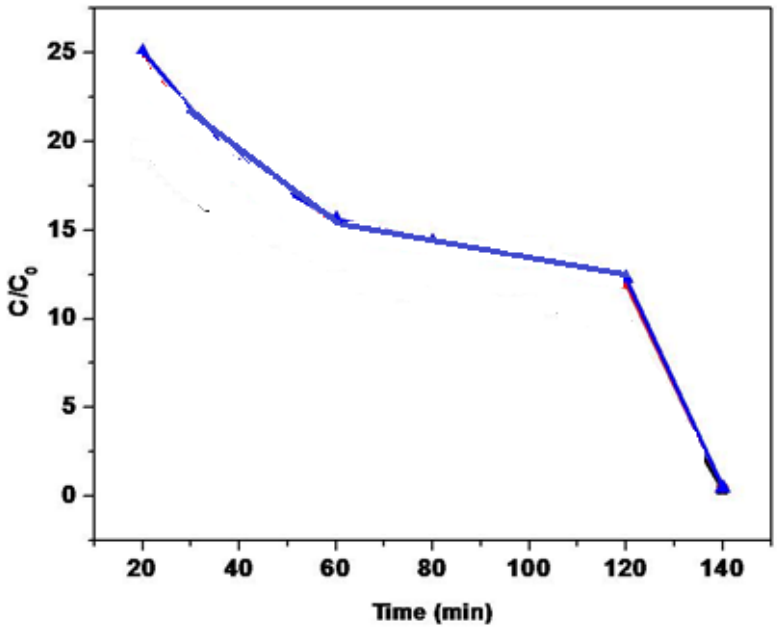

Figure 6b Variation of Photocatalytic degradation time in mine Vs (C/C_0)

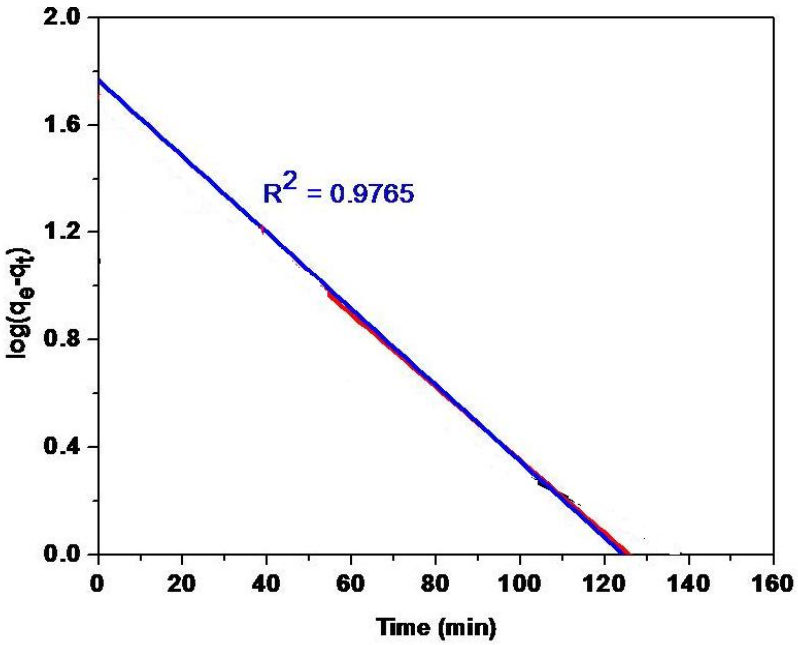

Figure 6c Variation of Photocatalytic degradation with respect to time

Table 3 Parameter and linear kinetic equations of Phototcatalytic reaction

Sample Dye MB	Initial concentration C (mg/L)	k - value	Pseudo first order kinetic equation	R^2
ZnO	10	0.0698 min^{-1}	$In(C/C_o)$= 0.0698t-0.5523	0.9801

IV. CONCLUSION

ZnO NPs were successfully prepared by hydrothermal process. The as-synthesized composites were characterized in terms of their structural and optical properties which revealed the well-crystalline nature and good Photocatalytic properties for as-synthesized products. ZnO plates are self-assembled together to form flower like structure. The photodegradation efficiency of MB with ZnO can reached to 98% after illumination for 60 min. ZnO nanorods possess electron storage properties which in turn facilitate to the separation of electron-hole pairs, therefore enhance the photocatalytic activity.

REFERENCES

[1] Yuan, J.; Choo, E.S.; Tang, X.; Sheng, Y.; Ding, J.; Xue, J. Synthesis of ZnO-Pt nanoflowers and their photocatalytic applications. *Nanotechnology*, **2010**;21:185606-185611

[2] Herzing, A.A.; Kiely, C.J.; Carley, A.F.; Landon, P.; Hutchings, G.J. Identification of active gold nanoclusters on iron oxide supports for co oxidation. *Science*, **2008**; 321: 1331-1335

[3] Zou, C.W.; Rao, Y.F.; Alyamani, A.; Chu, W.; Chen, M.J.; Patterson, D.A.; Emanuelsson, E.A.; Gao, W. Heterogeneous lollipop-like V_2O_5/ZnO array: a promising composite nanostructure for visible light photocatalysis. *Langmuir*, **2010**; *26*:11615-11620

[4] Li, Y.Z.; Xie, W.; Hu, X.L.; Shen, G.F.; Zhou, X.; Xiang, Y.; Zhao, X.J.; Fang, P.F. Comparison of Dye Photodegradation and its Coupling with Light-to-Electricity Conversion over TiO_2 and ZnO. *Langmuir*, **2010**; *26*: 591-597

[5] Murata, Y.; Fukuta, S.; Ishikawa, S.; Yokayama, S. Photoelectrochemical properties of TiO_2 rutile microalloyed with 4d and 5d transition elements. *Sol. Energy Mater. Sol. Cells*, **2000**; *62*:157-165

[6] Sakthivel, S.; Shankar, M.V.; Palanichamy, M.; Arabindoo, B.; Murugesan, V. Photocatalytic decomposition of leather dye Comparative study of TiO_2 supported on alumina and glass beads. *J. Photochem. Photobiol.* A, **2002**; 148:153-159

[7] Kaviyarasu, K., N. Geetha, K. Kanimozhi, C. Maria Magdalane, S. Sivaranjani, A. Ayeshamariam, J. Kennedy, and M. Maaza. "In vitro cytotoxicity effect and antibacterial performance of human lung epithelial cells A549 activity of zinc oxide doped TiO2 nanocrystals: investigation of bio-medical application by chemical method." *Materials Science and Engineering: C*, 2017; 74: 325-333.

[8] Saravanakkumar, D., S. Sivaranjani, K. Kaviyarasu, A. Ayeshamariam, B. Ravikumar, S. Pandiarajan, C. Veeralakshmi, M. Jayachandran, and M. Maaza. "Synthesis and characterization of ZnO–CuO nanocomposites powder by modified perfume spray pyrolysis method and its antimicrobial investigation." *Journal of Semiconductors* (2018); 39(3): 033001-033008.

[9] Geetha, N., S. Sivaranjani, A. Ayeshamariam, M. Siva Bharathy, S. Nivetha, K. Kaviyarasu, and M. Jayachandran. "High Performance Photo-Catalyst Based on Nanosized ZnO–TiO_2 Nanoplatelets for Removal of RhB Under Visible Light Irradiation." *Journal of Advanced Microscopy Research* , (2018); 13(1): 12-19.

[10] Gupta, T.K., Inhibition of grain growth in ZnO. *Journal of the American Ceramic Society*, 1971;*54*(8): 413-414.

[11] Heidari, A., Younesi, H. and Zinatizadeh, A.A.L., Controllable synthesis of flower-like zno nanostructure with hydrothermal method (research note). *International Journal of Engineering-Transactions B: Applications*, 2009; *22*(3): 283-290.

[12] Schunk, L.O. and Steinfeld, A. Kinetics of the thermal dissociation of ZnO exposed to concentrated solar irradiation using a solar-driven thermogravimeter in the 1800–2100 K range. *AIChE journal*, ., 2009; *55*(6): 1497-1504.

[13] Vidya, C., C. Manjunatha, M. N. Chandraprabha, Megha Rajshekar, and Antony Raj MAL. "Hazard free green synthesis of ZnO nano-photo-catalyst using Artocarpus Heterophyllus leaf extract for the degradation of Congo red dye in water treatment applications." *Journal of environmental chemical engineering*, (2017); 5(4): 3172-3180.

IOSR Journal of Engineering (IOSRJEN) is UGC approved Journal with Sl. No. 3240, Journal no. 48995.

D. Nathiya. "ZnO Nanorods and its Photocatalytic Studies on Methylene Blue Dye." IOSR Journal of Engineering (IOSRJEN), vol. 09, no. 06, 2019, pp. 28-34.